

**Coupled hydrodynamic and habitat suitability models  
jointly reveal suitable area for stock enhancement and  
release of marine organism larvae in Liaodong Bay**

**Xiaowei Hu<sup>1, #</sup>, Wenhao Hou<sup>2, #, \*</sup>, Zhaojun Sheng<sup>1, 3</sup>, Yanbin Xi<sup>4</sup>,  
Jiaxuan Yu<sup>1, 3</sup>, Ruijin Zhang<sup>1, 3, \*</sup>**

<sup>1</sup> College of Marine Science and Environment, Dalian Ocean University, Dalian, China

<sup>2</sup> State Key Laboratory of Coastal and Offshore Engineering, Dalian University of Technology, Dalian, China

<sup>3</sup> Operational Oceanographic Institution, Dalian Ocean University, Dalian, China

<sup>4</sup> National Marine Environmental Monitoring Center, Dalian, China

<sup>#</sup> These authors contributed equally to this work and share first authorship.

<sup>\*</sup> Corresponding author:

Wenhao Hou (hwhao0636@163.com)

Ruijin Zhang (ruijinz@dlou.edu.cn)

**Abstract**

Stock enhancement can effectively increase population sustainability and improve fishery resources, making it crucial to discern the suitable habitats for stock enhancement based on efficiency considerations. In this paper, a comprehensive model was established to simulate environmental characteristics in the Liaodong Bay. A habitat suitability model was developed by considering the optimal growth conditions of the *Portunus trituberculatus* larvae (PTL). The coupled model showed that the optimal area for stock-enhancement with PTL occurs in late June, and the initial suitable habitat area identified represents 17.12% of the whole Liaodong Bay. Based on the larval migration model of PTL, the deviation between the larvae and the

suitable habitat, as well as the actual available area for stock enhancement, were further determined after larval release in the initial suitable habitat. Only 33.67% of the larvae fulfilled the criteria of remaining within the suitable habitat for 95% of the time, and these larvae represented 6.19% of the whole area of Liaodong Bay. These findings means that the truly area available for stock enhancement is likely to be a very small portion of the entire bay, and more precise release of larvae will be necessary to ensure survival rates after release. Our study actually provides a methodological framework for the identification of suitable environment of stock enhancement. This methodology can provide technical guidance for the stock enhancement of marine larvae with same applicability for other bays, which in turn contributes to the sustainable use of marine ecosystem services and fisheries resources.

**Keywords:** Habitat suitability model; Fluid dynamics; Migration trajectory; Particle tracking; *Portunus trituberculatus*

## 1 Introduction

As overfishing, environmental pollution, and habitat destruction become increasingly serious, marine resources around the world are facing significant challenges (Etiegni et al., 2011; Horodysky et al., 2016; Utomo et al., 2019). Many countries have adopted fisheries management measures to address the current decline of marine fisheries resources, establishing controlling fishing quotas, marine reserves, and stock enhancement (Colloca et al., 2013; Green et al., 2014; Nielsen and Holm, 2007; Roberts et al., 2005). Among them, stock enhancement programs, with their effective ecosystem restoration function and advantage in alleviating the scarcity of fishery resources, are considered to be an important measure for restoring fishery resources (Han et al., 2016; Purcell et al., 2012; Taylor et al., 2005; Wang et al.,

2022). Stock enhancement refers to the artificial release of fish, shrimp, shellfish, algae, and other aquatic organisms into natural waters to allow for their natural growth, in order to increase the population size of marine species, rebuilt biomass of the fished stock, attempting to restore ecological balance (Hilborn et al., 2020; Lorenzen et al., 2010; Pilnick et al., 2021).

In the late 19th century, breakthroughs in artificial breeding technology for marine fish allowed countries such as the United States, Japan, and some European nations to establish marine fish hatcheries (Christou et al., 2013; Shelbourne, 1964; Yoshimura et al., 1996). Economically valuable species such as *Gadus* and *Oncorhynchus keta* were artificially propagated, and attempts were made to increase the wild populations in natural water bodies by releasing hatchery-reared fish (Blankenship and Leber, 1995; Kitada, 2014). Since the 1950s, China has been exploring stock enhancement activities in its nearshore fisheries (Dong et al., 2009). In the early 1980s, China's efforts in stock enhancement and large-scale larva release experiments in its nearshore fisheries have continuously achieved success (Han et al., 2016; Hong and Zhang, 2002). The *Portunus trituberculatus*, with its high reproductive potential, survival rates, high economic profitability, and the technology of artificial breeding, has been identified as a key organism for stock enhancement and release in China's northern waters, particularly in the Liaodong Bay, China (Wang et al., 2020). However, the efficiency of stock enhancement has long been at a low level due to incomplete identification of oceanic environmental factors (such as tidal currents) (Wang et al., 2017). Some studies have suggested that larvae released during stock enhancement programs are vulnerable to extreme physical factors, such as typhoon waves, which can lead to high mortality rates (Gao et al., 2022). Ensuring the survival rate of released larvae in natural marine habitats has been

76 challenging (Wang et al., 2018; Xie et al., 2014). Thus, it is crucial to efficiently  
77 describe tidal currents, temperature, salinity, and wave conditions in the releasing area,  
78 to determine suitable areas for larval survival.

79 In the turn of the century, the fishing industry and researchers made easier to  
80 identify environmental characteristics of fish culture and release areas by using  
81 remote monitoring systems with integrated temperature and salinity sensors  
82 (Laroche et al., 2016; Lee et al., 2022; Skålvik et al., 2023). However, when faced  
83 with the need to understand the environmental features of larger oceanic areas, this  
84 technology becomes increasingly difficult to implement, as larger areas require more  
85 equipment and personnel investment, leading to a significant growing in production  
86 costs. In recent years, with the continuous development and improvement of ocean  
87 mathematical models, an increasing number of researchers utilized numerical  
88 simulation techniques to estimate the environmental characteristics of large marine  
89 areas (Karydis and Kitsiou, 2013; Ma et al., 2023; Uzun et al., 2022). The  
90 advantages of mathematical models lie in their ability to provide rapid feedback of  
91 environmental features over a large area at a low cost. Therefore, this enabled the  
92 selection of suitable areas for stock enhancement through numerical modeling of basic  
93 environmental variables.

94 This study focused on the stock enhancement population, through the release of  
95 *Portunus trituberculatus* larvae (PTL) as a case of study. Firstly, a comprehensive  
96 numerical model of the water environment in the Liaodong Bay was developed, which  
97 took into account physical factors such as tidal currents, water temperature, salinity,  
98 and waves. Based on this, an environmental suitability model and migration model of  
99 PTL were established, aiming to identify through the assess suitable areas for the  
100 stock enhancement of PTL in the Liaodong Bay. The results of this study are expected

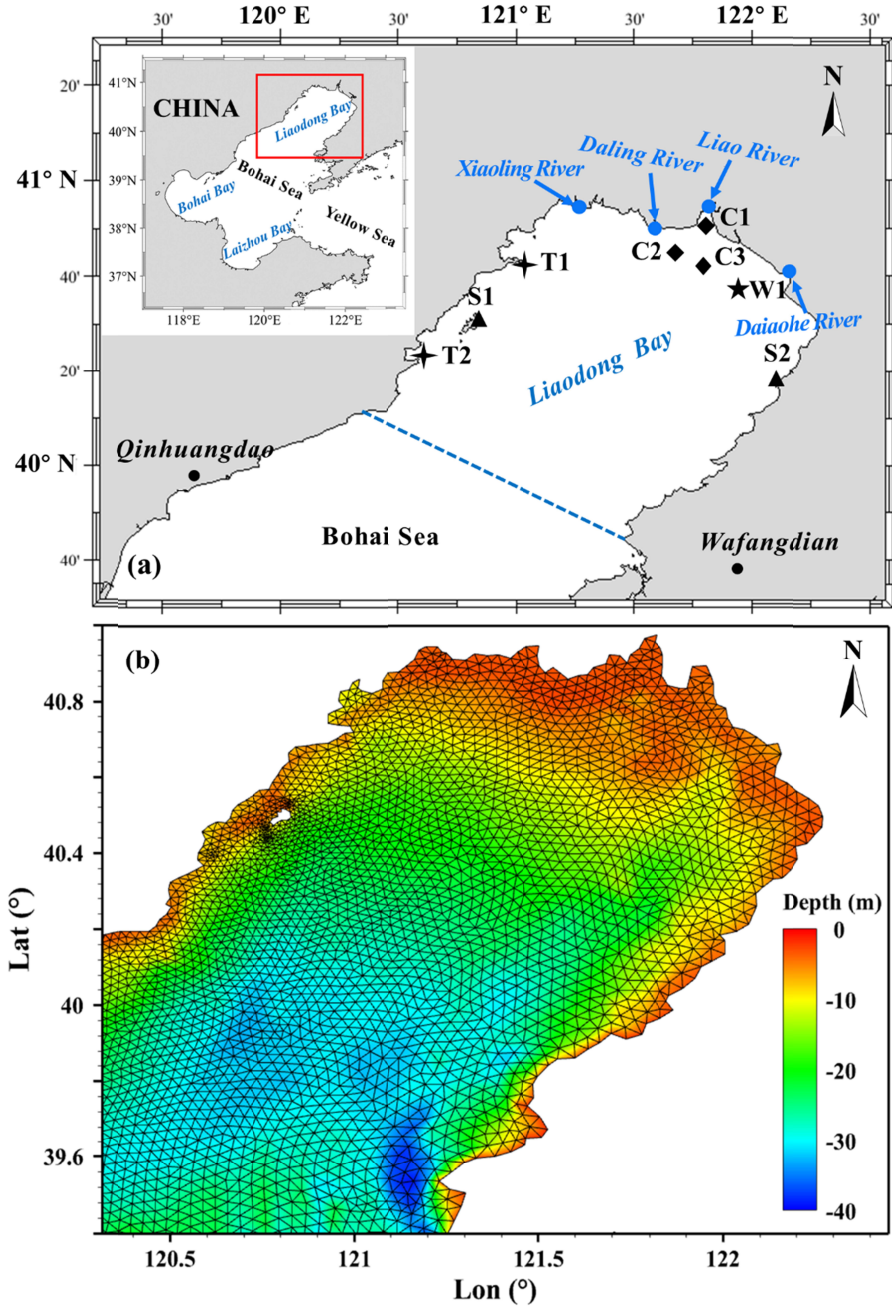


101 to provide effective guidance for the selection of stock enhancement and release areas,  
102 thereby facilitating the management, conservation, and sustainability of regional  
103 fisheries resources.

## 104 **2 Materials and Methods**

### 105 **2.1 Study area**

106 The study area is located in the Liaodong Bay, China (Figure 1. (a)), one of the  
107 main areas for stock enhancement in the Bohai Sea, with a sea area of 18,784.53 km<sup>2</sup>.  
108 The Liaodong Bay is situated in the northern part of the Bohai Sea, with an average  
109 water depth of 18 m. The bay is influenced by irregular semidiurnal tides, with an  
110 average tidal range of 2.7 m. It is one of the most important spawning and breeding  
111 grounds for many commercially valuable marine species, such as *Portunus*  
112 *trituberculatus* and *Penaeus orientalis* (Wang et al., 2013; Xu et al., 2010). The  
113 average annual water temperature in the bay ranges from 8 to 10°C. The sea-ice  
114 season typically begins in December and ends in March of the following year, with an  
115 average duration of 112 days per year (Hou et al., 2020; Wang et al., 2021). The  
116 main species for aquaculture release in Liaodong Bay are *Portunus trituberculatus*,  
117 Chinese shrimp and *Paralichthys olivaceus*. Taking the PTL as an example, the  
118 window for stock enhancement and release is from June to July each year. This is  
119 because the larvae are prone to freeze and die before this period, while later releases  
120 may not be harvested before the onset of the ice season. In addition, the stock  
121 enhancement and release is usually carried out during the neap tide period due to the  
122 relatively stable marine environment compared to the spring tide period. With this in  
123 mind, this study focuses primarily on four neap tide periods occurring in June and  
124 July of 2019, namely, early June, late June, early July, and late July.



126

128 **Figure 1.** (a) Location of study area and distribution of observation stations. (b) The  
 129 water depth and computational grids of the Liaodong Bay.

## 129 2.2 Habitat environment model of *Portunus trituberculatus* larvae (PTL)

131 Given the importance of the habitat characteristics of PTL in the context of its  
 132 stock enhancement and release, a numerical model of the marine water environment

131 in the Liaodong Bay was developed in this study. The general model consisted of a  
 132 three-dimensional hydrodynamic model to reproduce the tidal characteristics of the  
 133 Liaodong Bay, a three-dimensional temperature and salinity model to simulate the  
 134 distribution of water temperature and salinity in the Liaodong Bay, and a wave model  
 135 to reflect the wave propagation characteristics in the Liaodong Bay. The  
 136 hydrodynamic model was based on the Reynolds-averaged Navier-Stokes equations  
 137 (RANS) simplified under the assumption of static water. The governing equations of  
 138 the hydrodynamic model are as follows:

$$139 \quad \frac{\partial u}{\partial x} + \frac{\partial v}{\partial y} + \frac{\partial w}{\partial z} = S \quad (1)$$

$$140 \quad \begin{aligned} & \frac{\partial u}{\partial t} + \frac{\partial u^2}{\partial x} + \frac{\partial vu}{\partial y} + \frac{\partial wu}{\partial z} = fv - g \frac{\partial \eta}{\partial x} - \frac{1}{\rho_0} \frac{\partial p_a}{\partial x} - \\ & \frac{g}{\rho_0} \int_z^\eta \frac{\partial \rho}{\partial x} dz - \frac{1}{\rho_0 h} \left( \frac{\partial s_{xx}}{\partial x} + \frac{\partial s_{xy}}{\partial y} \right) + F_u + \frac{\partial}{\partial z} \left( v_t \frac{\partial u}{\partial z} \right) + u_s S \end{aligned} \quad (2)$$

$$141 \quad \begin{aligned} & \frac{\partial v}{\partial t} + \frac{\partial v^2}{\partial y} + \frac{\partial uv}{\partial x} + \frac{\partial wv}{\partial z} = -fu - g \frac{\partial \eta}{\partial y} - \frac{1}{\rho_0} \frac{\partial p_a}{\partial y} - \\ & \frac{g}{\rho_0} \int_z^\eta \frac{\partial \rho}{\partial y} dz - \frac{1}{\rho_0 h} \left( \frac{\partial s_{yx}}{\partial x} + \frac{\partial s_{yy}}{\partial y} \right) + F_v + \frac{\partial}{\partial z} \left( v_t \frac{\partial v}{\partial z} \right) + v_s S \end{aligned} \quad (3)$$

142 where  $t$  is the time;  $x, y$  are Cartesian coordinate system coordinates;  $\eta$  is the surface  
 143 elevation;  $d$  is the still water depth;  $h = \eta + d$  is the total water depth;  $u, v$  and  $w$  are  
 144 the velocity components in  $x, y$  and  $z$  directions respectively;  $f$  is the Coriolis force  
 145 coefficient,  $f = 2\omega \sin \varphi$  ( $\omega$  is the angular rate of revolution,  $\varphi$  is the local latitude);  $g$  is  
 146 the acceleration of gravity;  $\rho$  is the density of water;  $S_{xx}, S_{xy}$  and  $S_{yx}$  are components of  
 147 the radiation stress tensor;  $v_t$  is the vertical turbulent (or eddy) viscosity;  $p_a$  is the  
 148 atmospheric pressure;  $\rho_0$  is the reference density of water.  $S$  is the magnitude of the  
 149 discharge due to point sources and  $(u_s, v_s)$  is the velocity by which the water is  
 150 discharged into the ambient water.

151 The model presented in this study utilized a non-structured triangular mesh  
 152 (Figure 1 (b)), consisting of 14,002 grid elements with a minimum resolution of 100  
 153 meters for nearshore areas. The depth and shoreline data used in the model were  
 154 obtained from the ETOPO1 database provided by the National Oceanic and  
 155 Atmospheric Administration (NOAA). In addition, the model accounted for four  
 156 major rivers (the Liao River, the Daliao River, the Daling River, and the Xiaoling  
 157 River) flowing into the Liaodong Bay, with monthly discharge data provided for each.  
 158 The predicted tidal level obtained through harmonic analysis was used to provide the  
 159 open boundary tidal condition.

160 Apart from the influence of current, water temperature and salinity are also  
 161 significant factors that cannot be ignored in the growth of PTL (Dai et al., 2014; Xu  
 162 and Liu, 2011). Based on the validated hydrodynamic model, another model was  
 163 established to simulate the temperature and salinity distribution characteristics of the  
 164 Liaodong Bay. The temperature and salinity boundary conditions were provided by  
 165 monthly average data from the Copernicus Marine Environment Monitoring Center  
 166 website (<https://marine.copernicus.eu/>). The model control equations are as follows:

$$167 \quad \frac{\partial T}{\partial t} + \frac{\partial uT}{\partial x} + \frac{\partial vT}{\partial y} + \frac{\partial wT}{\partial z} = F_T + \frac{\partial}{\partial z} \left( D_v \frac{\partial T}{\partial z} \right) + \hat{H} + T_s S \quad (4)$$

$$168 \quad \frac{\partial s}{\partial t} + \frac{\partial us}{\partial x} + \frac{\partial vs}{\partial y} + \frac{\partial ws}{\partial z} = F_s + \frac{\partial}{\partial z} \left( D_v \frac{\partial s}{\partial z} \right) + s_s S \quad (5)$$

169 where  $D_v$  is the vertical turbulent (eddy) diffusion coefficient.  $\hat{H}$  is a source term  
 170 due to heat exchange with the atmosphere.  $T_s$  and  $s_s$  are the temperature and the  
 171 salinity of the source.

172 On the basis of temperature and salinity, the food source depletion and flow field  
 173 heterogeneity caused by wave breaking are potential factors affecting the migration  
 174 and distribution of marine organisms (Hou et al., 2022). Therefore, the MIKE21-SW

175 model was used to calculate the wave characteristics in the Liaodong Bay, which  
 176 takes into account meteorological conditions such as wind speed and provides the  
 177 distribution of the significant wave height in the Liaodong Bay, which is widely used  
 178 for wave characteristics simulation. The background wind field used meteorological  
 179 data from the Copernicus Marine Environment Monitoring Officer website  
 180 (<https://marine.copernicus.eu/>). The model control equations are as follows:

$$181 \quad \frac{\partial N}{\partial t} + \nabla \cdot (\vec{V}N) = \frac{S}{\sigma} \quad (6)$$

182 where  $N(\vec{x}, \sigma, \theta, t)$  is the action density,  $t$  is the time,  $\vec{x} = (x, y)$  is the Cartesian  
 183 co-ordinates;  $\vec{V} = (c_x, c_y, c_\theta, c_\sigma)$  is the propagation velocity of a wave group in the  
 184 four-dimensional phase space  $\vec{x}, \sigma, \theta$  and  $S$  is the source term for the energy balance  
 185 equation.

186 The energy source term,  $S$ , represents the superposition of source functions  
 187 describing various physical phenomena.

$$188 \quad S = S_{in} + S_{nl} + S_{ds} + S_{bot} + S_{surf} \quad (7)$$

189 where  $S_{in}$  represents the transmission of energy by wind,  $S_{nl}$  is the wave energy  
 190 transfer due to non-linear wave-wave interaction,  $S_{ds}$  is the dissipation of wave  
 191 energy due to whitecapping,  $S_{bot}$  is the dissipation due to the bottom friction and  
 192  $S_{surf}$  is the dissipation of wave energy due to the depth-induced breaking.

### 193 **2.3 Habitat suitability model for *Portunus trituberculatus* larvae (PTL)**

194 Previous studies have shown that fluid shear stress caused by waves and tides  
 195 affects the transport, attachment and recruitment of marine organism larvae (Bolle et  
 196 al., 2009; Hou et al., 2022; Reidenbach et al., 2009; Shanks et al., 2003; Whitman and  
 197 Reidenbach, 2012), while water temperature and salinity directly affect larval feeding

198 and development (McGeady et al., 2021; Nurdiani and Zeng, 2007; Zimmerman and  
 199 Pechenik, 1991). Existing research and the Chinese technical specifications for the  
 200 stock enhancement indicate the appropriate growth conditions for PTL (China, 2014;  
 201 Ge, 2019; Wang et al., 2022), as shown in the Table 1 below.

202 **Table 1.** Suitable growth conditions for PTL

Environmental factors	Suitable range
Water temperature (°C)	16 ~ 28
Salinity (‰)	20 ~ 32
Velocity (m/s)	< 1.0
Significant wave height (m)	< 0.5

203 In the suitability model for the habitat of PTL, it is initially believed that flow  
 204 velocity, water temperature, salinity, and significant wave height are the main limiting  
 205 factors for the habitat of PTL. The single-factor Habitat Suitability Index (*HSI*) was  
 206 used to quantify the suitability of the target organism in a particular factor. The *HSI*  
 207 ranges from 0 (least suitable) to 1 (most suitable), indicating that the factor has no  
 208 restriction on the survival of the target organism when the *HSI* index is 1. The  
 209 Comprehensive Suitability Index (*CSI*) was calculated based on the *HSI* of each  
 210 habitat factor and the main limiting factors for the survival of the organism. The *CSI*  
 211 ranges from 0 to 1. In this assessment, it was considered that larvae could settle and  
 212 survive when the *CSI* was greater than 0.95. The single-factor habitat suitability index  
 213 (*HSI*) and the comprehensive suitability index (*CSI*) of the larvae on the day of stock  
 214 enhancement can be expressed as:

215 
$$HSI(V_i, Tem_i, Sat_i, SWH_i) = \frac{t_i(V_i, Tem_i, Sat_i, SWH_i)}{24} \quad (8)$$

$$CSI(HSI_{V_i}, HSI_{Tem_i}, HSI_{Sat_i}, HSI_{SWH_i}) = \frac{1}{n} (HSI_{V_i} + HSI_{Tem_i} + HSI_{Sat_i} + HSI_{SWH_i}) \quad (9)$$

where  $i$  is the  $i$ -th grid cell,  $t_i$  is the total time in the  $i$ -th grid cell that a single suitable condition is met within a day;  $n$  is the number of habitat factors that affect the growth of individual organisms;  $V_i$ ,  $Tem_i$ ,  $Sat_i$  and  $SWH_i$  are the flow velocity, water temperature, salinity and significant wave height, respectively, which are environmental factors characterizing the unit  $i$ . These features are calculated by the habitat environment model.  $HSI_{V_i}$ ,  $HSI_{Tem_i}$ ,  $HSI_{Sat_i}$  and  $HSI_{SWH_i}$  are the habitat suitability index based on flow velocity, water temperature, salinity and significant wave height at unit  $i$ , respectively.

The Weighted Usable Area ( $WUA$ ) is calculated by simulating the suitability of larvae to hydrological factors. Specifically,  $WUA$  is defined as the summation of the product of the area of each control unit ( $a_i$ ) and the  $CSI$  within the study region.

$$WUA = \sum_{i=1}^n CSI(HSI_{V_i}, HSI_{Tem_i}, HSI_{Sat_i}, HSI_{SWH_i}) a_i \quad CSI > 0.95 \quad (10)$$

## 2.4 Migration model of *Portunus trituberculatus* larvae (PTL)

During the early stage of stock enhancement and release, the movement of PTL is largely determined by ocean currents, due to their small size and weak self-swimming ability (Ge, 2019; Ma et al., 2021). To predict the migration and distribution of the larvae, we developed a particle tracking numerical model. This model considers the larvae as particles (600 in total) moving in dependence on the water mass points. After being released within the initial suitable area identified by the habitat suitability model, the transport and diffusion of the larvae follows the following principles:

$$dX_t = a(t, X_t) dt + b(t, X_t) \xi_t \quad (11)$$

239 where  $a$  is the drift term;  $b$  is the diffusion term;  $\xi$  is the random number. To  
 240 compute the trajectory of  $Y$  for a given time discretization, we set the initial value as  
 241  $Y_0 = X_0$  and recursively solve for  $Y$  using the following equation.

$$242 \quad dY_{n+1} = Y_n + a(t, X_t)Y_n\Delta_n + b(t, X_t)Y_n\Delta W_n \quad (12)$$

243 where  $n=1, 2, 3, \dots$ , the value of  $n$  is contingent upon the Euler drift coefficient  $a$  and  
 244 the diffusion coefficient  $b$ .  $\Delta W = W_t - W_s \in N(\mu = 0, \sigma^2 = \Delta_n)$  is within the  
 245 continuous time period ( $\tau_n \leq t \leq \tau_{n+1}$ ), based on the Gaussian increment of the Wiener  
 246 process.

247 We utilized a particle tracking model to assess the migration characteristics of  
 248 larvae and the likelihood of their persistence within suitable habitats during a  
 249 specified duration following their release.

## 250 **2.5 Error statistics**

251 The root mean square error (RMSE) is a commonly used evaluation metric for  
 252 testing the reliability of models.

$$253 \quad RMSE = \sqrt{\frac{1}{N} \sum_{i=1}^N (S_i - O_i)^2} \quad (13)$$

254 where  $S_i$  is the modeling series,  $O_i$  is the observation series, and  $N$  is the total  
 255 number of data in the series. Given that error measures may not always be indicative  
 256 of optimal performance for numerical models that simulate natural phenomena such  
 257 as atmospheric dynamics, ocean circulation, or wave generation and propagation, the  
 258 concept of the skill model has been introduced to enhance evaluation (Hou et al.,  
 259 2021).



$$skill = 1 - \frac{\sum_{i=1}^N |M - D|^2}{\sum_{i=1}^N (|M - \bar{D}| + |D - \bar{D}|)^2} \quad (14)$$

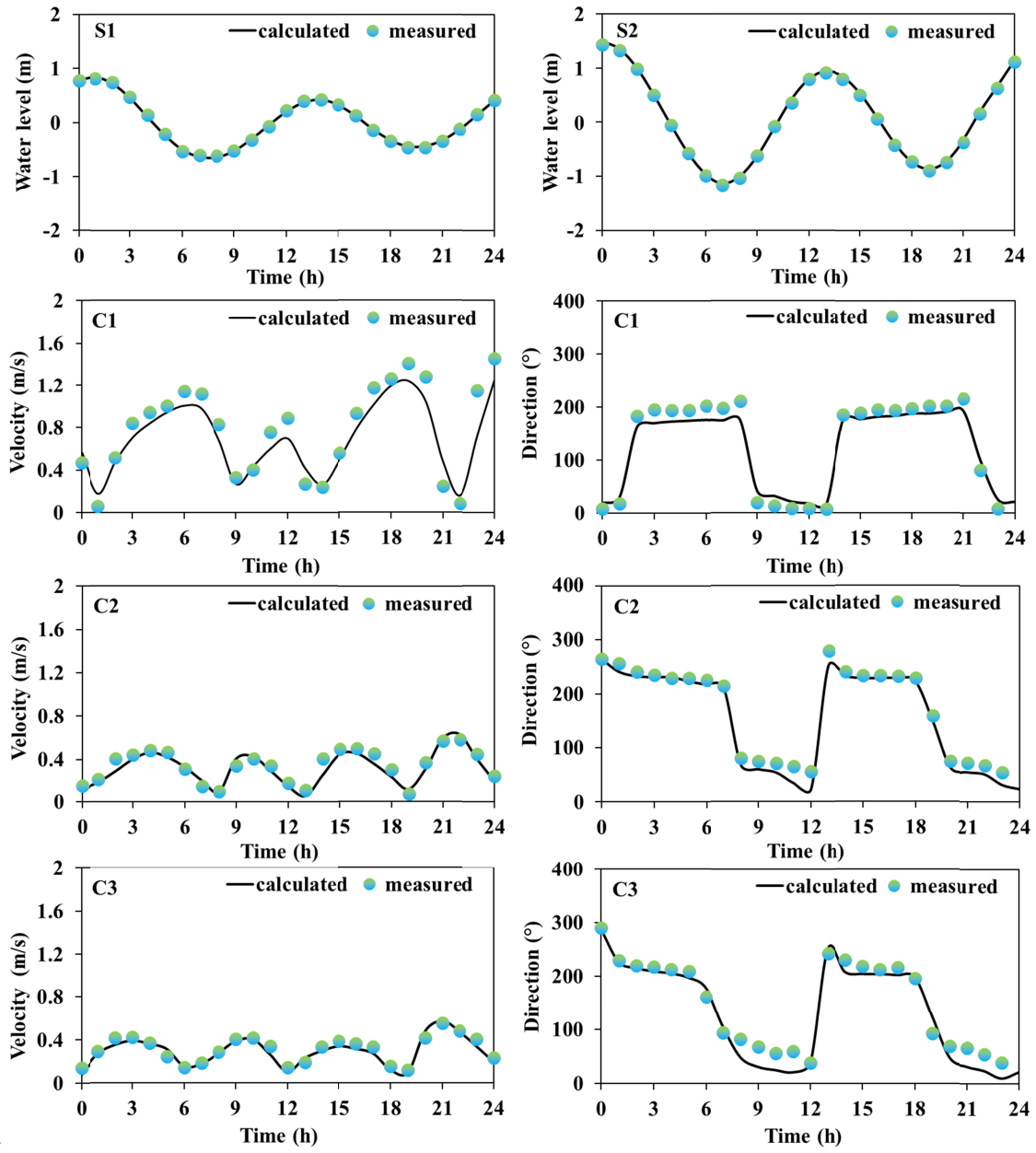
where  $M$  is the modeling series,  $D$  is the observation series,  $\bar{D}$  is the average of the observation data, and  $N$  is the total number of data in the series. Performance levels are categorised as: larger than 0.65 excellent; between 0.65 and 0.5 very good; between 0.5 and 0.2 good; smaller than 0.2 poor.

### 3 Results

#### 3.1 Model validation and results analysis

A series of field data were initially collected for the validation of the model reliability, which included tide gauge data from two stations (S1, and S2) obtained from continuous 25-hour measurements on May 25, 2022, provided by the China National Marine Information Center; current data from three stations (C1, C2, and C3) measured using a current meter on September 18, 2021; water temperature and salinity from monthly average data from two stations (T1 and T2) for 2021, obtained from the Copernicus Marine Service website (<https://marine.copernicus.eu/>); and wave data from one station (W1), obtained from a fixed acoustic wave gauge over a 30-hour continuous observation period on May 14, 2016.

Based on the comparison between the on-site observation data and the results obtained from model calculations (Figure 2 and Figure 3), it can be concluded that the modeled tidal flow values are consistent with the characteristics of tidal propagation under natural conditions. The simulated results of sea water temperature, salinity, and waves were also found to be in good agreement with the measured data.



28:

283

**Figure 2.** Tidal current validation process

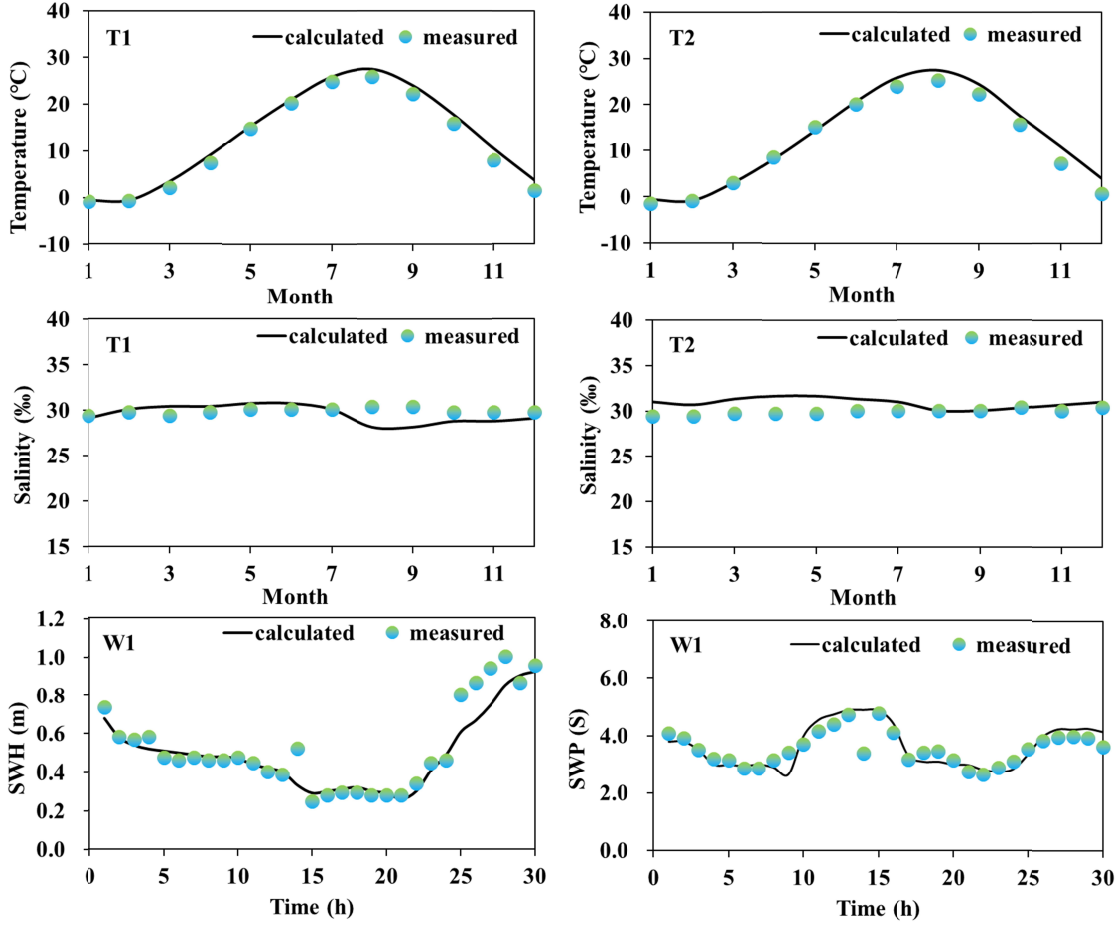


**Figure 3.** Water temperature, salinity and wave validation process

The results of the error analysis (Table 2) indicate that the calculated root mean square error (RMSE) of the tidal level has an average value of 0.08 m, while the RMSE of the flow velocity and flow direction has an average value of 0.07 m/s and 15.61°, respectively. The RMSE of the water temperature and salinity are 1.05°C and 1.21‰, respectively. The RMSE of the significant wave height and period are 0.11 m and 0.08 s, respectively. Overall, the observed and simulated values show good agreement, and the RMSEs are within an acceptable range. In addition, the skill model evaluation results for the tidal level, flow velocity, temperature, salinity, significant wave height (SWH), and significant wave period (SWP) are 0.93, 0.90, 0.90, 0.91, 0.88, and 0.90, respectively, indicating excellent performance of the

295 established habitat environment model. Consequently, we conclude that the  
 296 established numerical model was capable of describing the water environment  
 297 characteristics (tidal flow, water temperature, salinity, and waves) in the Liaodong  
 298 Bay.

299 **Table 2.** Statistical analysis of model errors

Item	Stations	RMSE	<i>skill</i>
Water level (m)	S1	0.07	0.94
	S2	0.09	0.92
	C1	0.10	0.85
Velocity (m/s)	C2	0.05	0.93
	C3	0.06	0.92
	C1	17.21	0.89
Direction (°)	C2	13.25	0.92
	C3	16.36	0.91
	T1	0.91	0.92
Temperature (°C)	T2	1.18	0.88
	T1	1.20	0.92
Salinity (‰)	T2	1.22	0.90
	T1	1.20	0.92
Significant wave hight (m)	W1	0.11	0.88
Significant wave period (s)	W1	0.08	0.90

### 300 **3.2 Habitat characteristics of *Portunus trituberculatus* larvae (PTL)**

301 According to the joint calculation results of the numerical model of water  
 302 environment and the habitat suitability model in the Liaodong Bay (Figure 4), the

303 habitat suitability index of flow velocity ( $HSI_v$ ) in the Liaodong Bay during the four  
304 neap tide periods showed a gradual increase from the sea to the land. Among them,  
305 the flow velocity suitability index of the coastal waters on the north side of Liaodong  
306 Bay was generally above 0.95, and other suitable areas were sporadically distributed  
307 in shallow waters on both sides of Liaodong Bay, where the flow velocity was  
308 relatively low due to the dampening effect of topographical factors. In the  
309 southeastern waters of Liaodong Bay, the flow velocity suitability index was less than  
310 0.20. This was mainly due to the large flow velocity caused by the water depth  
311 exceeding 30 meters and the tortuous coastline. The habitat environment model  
312 results showed that the maximum flow velocity in this area during the four periods is  
313 1.87 m/s, which occurred in early June.

314 Under flow velocity constraints, the optimal growth area for PTL in late June  
315 was found to be the largest, approximately 1488.06 km<sup>2</sup>, accounting for 7.92% of the  
316 total area of Liaodong Bay. Conversely, the optimal area was found to be the smallest  
317 in early June, at approximately 1337.49 km<sup>2</sup>, accounting for 7.12% of the total area.  
318 The suitable area in early July was 1371.96 km<sup>2</sup> and in late July was 1472.04 km<sup>2</sup>, and  
319 the flow rate suitable area accounted for about 7.30% and 7.84% of the whole  
320 Liaodong Bay area, respectively. It is evident that under the influence of tidal current  
321 stress, the habitat in late June is relatively more conducive to the growth of PTL.

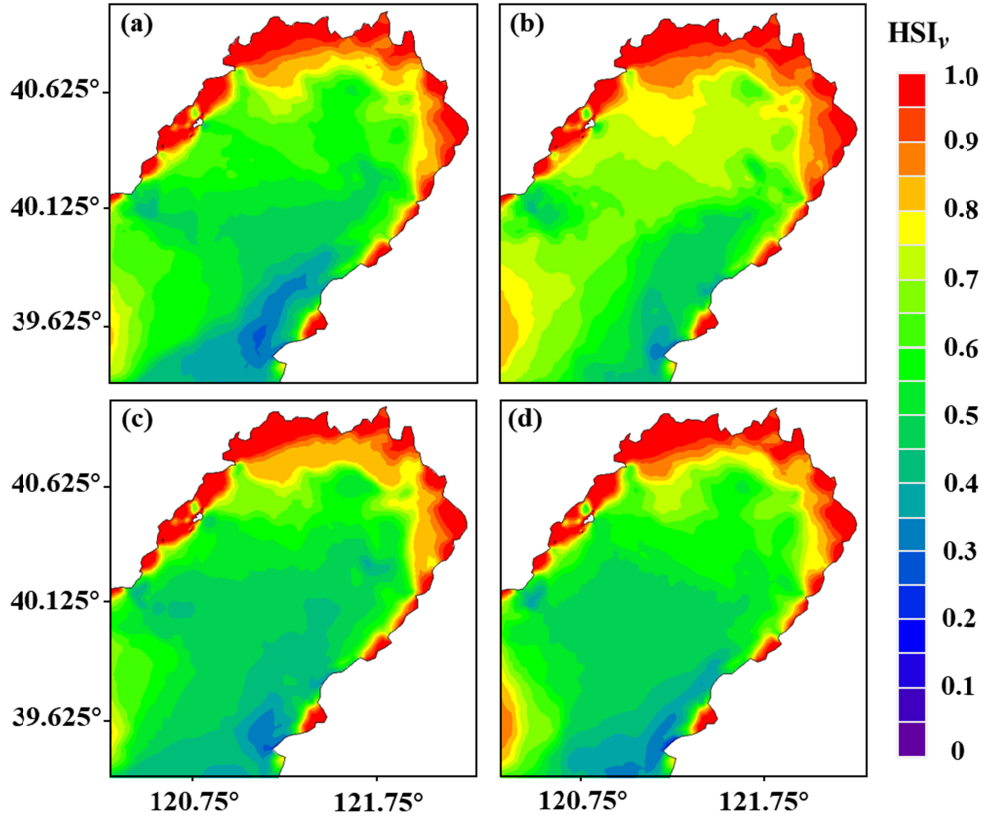
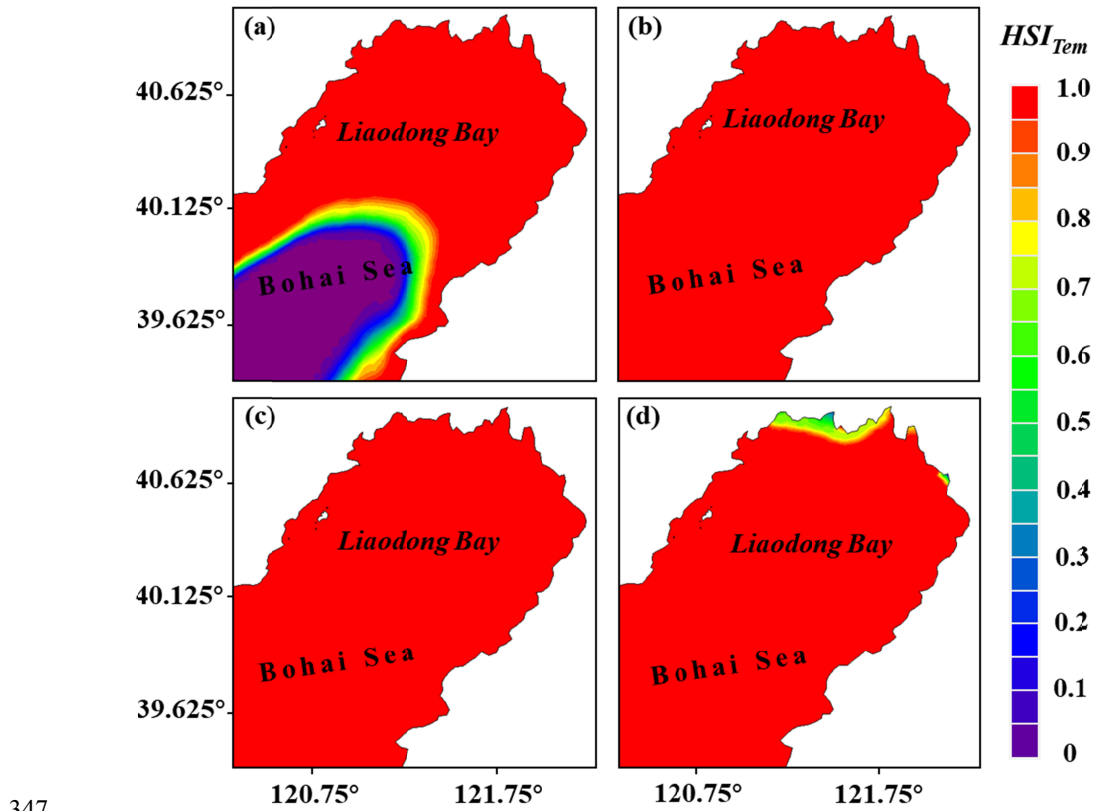


**Figure 4.** Distribution of the habitat suitability index for flow velocity ( $HSI_v$ ) during various periods in the Liaodong Bay. (a) Early June. (b) Late June. (c) Early July. (d) Late July.

The computational model results showed apparent temporal variations in water temperature within the Liaodong Bay. The water temperature exhibited a significant increase from June to July. At the spatial scale, the water temperature gradually decreased from the land towards the ocean. The suitability analysis results (Figure 5) indicated that there were unfavorable temperatures for the growth of PTL in the early June and late July, while the habitat suitability index of water temperature ( $HSI_{Tem}$ ) for the entire Liaodong Bay was 1.0 in late June and early July, indicating that water temperature was highly suitable for the growth of PTL in late June and early July.

In early June, the water temperature in the southern waters of the Liaodong Bay

346 was below 16°C, which limited the growth of the PTL, resulting in  $HSI_{Tem}$  of less  
 347 than 0.1 in the region. However, in late July, the water temperature in the nearshore  
 348 waters of the northern part of the Liaodong Bay exceeded 28°C. At this time, the  
 349 excessively high temperature impaired to the growth of the PTL. As a result, the  
 350 suitability index for this area was lower. Under the constraint of water temperature, in  
 351 early June, the suitable growth area for the PTL was 11873.52 km<sup>2</sup>, accounting for  
 352 63.21% of the entire Liaodong Bay area. In late July, the suitable growth area for the  
 353 PTL was 18591.48 km<sup>2</sup>, accounting for 98.97% of the entire Liaodong Bay area. In  
 354 late June and early July, the proportion of suitable area reached 100%. Therefore, it  
 355 can be seen that under high temperatures, the entire Liaodong Bay is suitable for the  
 356 growth of the PTL in late June and early July.



347 **Figure 5.** Distribution of the habitat suitability index for water temperature ( $HSI_{Tem}$ )  
 348

348 during various periods in the Liaodong Bay. (a) Early June. (b) Late June. (c) Early  
349 July. (d) Late July.

350 According to the distribution of the suitability index for salinity ( $HSI_{Sat}$ ), the  
351 majority of the areas in the Liaodong Bay were highly suitable for the growth of PTL.  
352 The areas with lower suitability were mainly located in the coastal waters on the north  
353 and south sides of the Liaodong Bay. In the nearshore areas on the northern side of the  
354 Liaodong Bay, the influx of freshwater from rivers resulted in localized areas of water  
355 with a salinity of less than 20‰. On a temporal scale, the  $HSI_{Sat}$  was inversely  
356 proportional to the river discharge (Table 3). In early June, the relatively low river  
357 discharge led to relatively high salinity levels in the estuarine area. In early June, the  
358 relatively small river discharge resulted in relatively higher salinity in the estuarine  
359 area. However, with the onset of the rainy season, the increasing river discharge  
360 gradually reduced the salinity in the nearshore estuarine area, with the maximum river  
361 discharge in late July resulting in the lowest  $HSI_{Sat}$  in the northern nearshore area of  
362 Liaodong Bay. In contrast, on the southern side of Liaodong Bay, due to the deeper  
363 water depth, the salinity exceeds 32‰, which limited the growth of PTL.

364 **Table 3.** Multi-year monthly average runoff of four major rivers in Liaodong Bay

	Liao River	Daliao River	Daling River	Xiaoling River
Early June	$1.85 \times 10^8 \text{ m}^3$	$1.88 \times 10^8 \text{ m}^3$	$0.28 \times 10^8 \text{ m}^3$	$0.02 \times 10^8 \text{ m}^3$
Late June	$2.43 \times 10^8 \text{ m}^3$	$2.10 \times 10^8 \text{ m}^3$	$0.31 \times 10^8 \text{ m}^3$	$0.03 \times 10^8 \text{ m}^3$
Early July	$2.01 \times 10^8 \text{ m}^3$	$3.16 \times 10^8 \text{ m}^3$	$0.25 \times 10^8 \text{ m}^3$	$0.24 \times 10^8 \text{ m}^3$
Late July	$2.17 \times 10^8 \text{ m}^3$	$3.34 \times 10^8 \text{ m}^3$	$0.28 \times 10^8 \text{ m}^3$	$0.25 \times 10^8 \text{ m}^3$

365 Under salinity restriction, the optimal growth area of PTL was largest in late June



(Figure 6), with an area of approximately 18775.53 km<sup>2</sup>, accounting for 99.95% of the entire Liaodong Bay. In early June, the optimal growth area was approximately 18740.61 km<sup>2</sup>, while in early July, it was approximately 18772.20 km<sup>2</sup>, and in late July, it was approximately 18646.65 km<sup>2</sup>, accounting for 99.77%, 99.93%, and 99.27% of the entire Liaodong Bay, respectively. Overall, the salinity of water in Liaodong Bay had little effect on the growth of PTL in June and July.

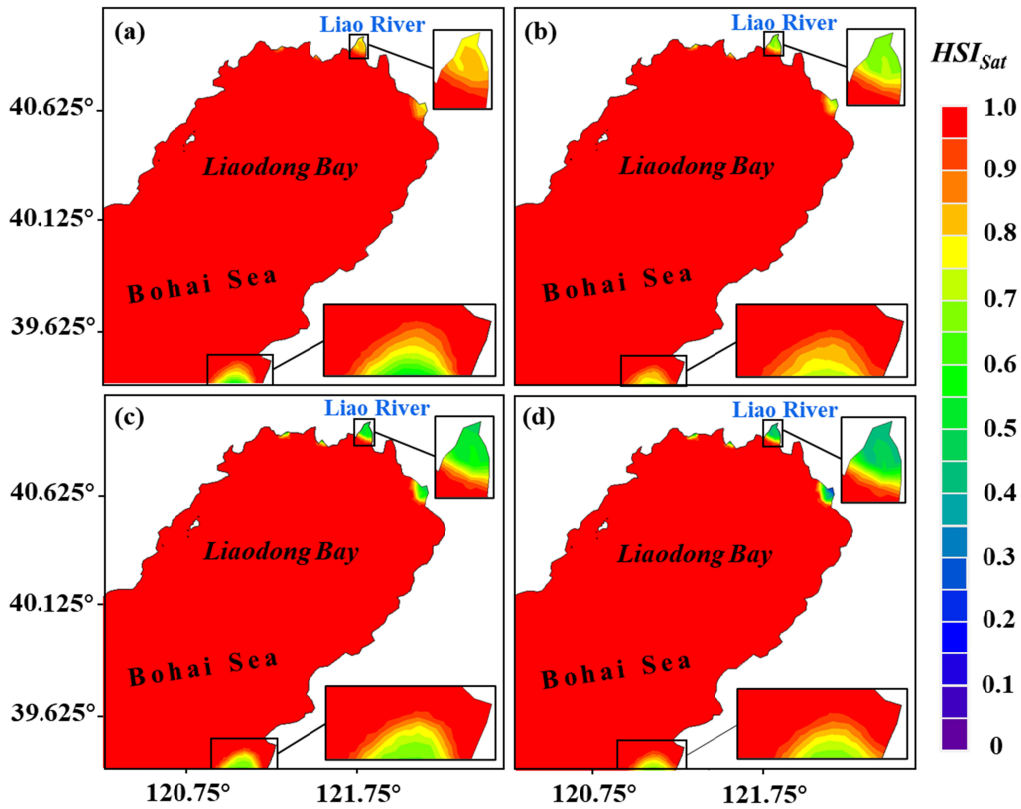


**Figure 6.** Distribution of the habitat suitability index for water salinity ( $HSI_{Sat}$ ) during various periods in the Liaodong Bay. (a) Early June. (b) Late June. (c) Early July. (d) Late July.

When considering the growth restriction of PTL by waves alone, we found that the suitability index for waves ( $HSI_{SWH}$ ) in the Liaodong Bay was 1 in all four periods, meaning that the significant wave height (SWH) was less than 0.5 m. This indicates

379 that wave conditions in the entire Liaodong Bay are suitable for larval growth during  
380 these four periods. Therefore, we regarded waves as a non-primary limiting factor  
381 when calculating the comprehensive suitability index (*CSI*).

### 382 **3.3 Suitable growth areas for *Portunus trituberculatus* larvae (PTL)**

383 The results of the habitat suitability model (Figure 7) showed that under the  
384 combined effects of flow velocity, water temperature, salinity, the suitable areas for  
385 the stock enhancement of PTL were mainly distributed in the north of Liaodong Bay.  
386 In both June and July, the *CSI* of PTL showed a trend of gradually increase from sea  
387 to land. The *CSI* of nearshore areas generally exceeded 0.85, indicating that the  
388 milder natural conditions in nearshore areas were adequate for the survival of PTL.  
389 Based on the results of the *CSI*, the suitable growth area ( $CSI > 0.95$ ) for the PTL was  
390 more concentrated in late June, mainly in the northern waters of the Liaodong Bay.

391 In terms of suitable PTL growth area, it was largest in late June, reaching  
392  $3217.77 \text{ km}^2$ , while the suitable areas in early June, early July, and late July were  
393  $2503.89 \text{ km}^2$ ,  $2253.51 \text{ km}^2$ , and  $2121.73 \text{ km}^2$ , respectively. Therefore, it can be  
394 inferred, based on the consideration of the operational space for stock enhancement,  
395 the best period for stock enhancement is during the neap tide of late June because it  
396 presents the largest suitable area for such a purpose. Subsequently, we initially  
397 identified suitable area by determining those with a *CSI* greater than 0.95 in late  
398 June.

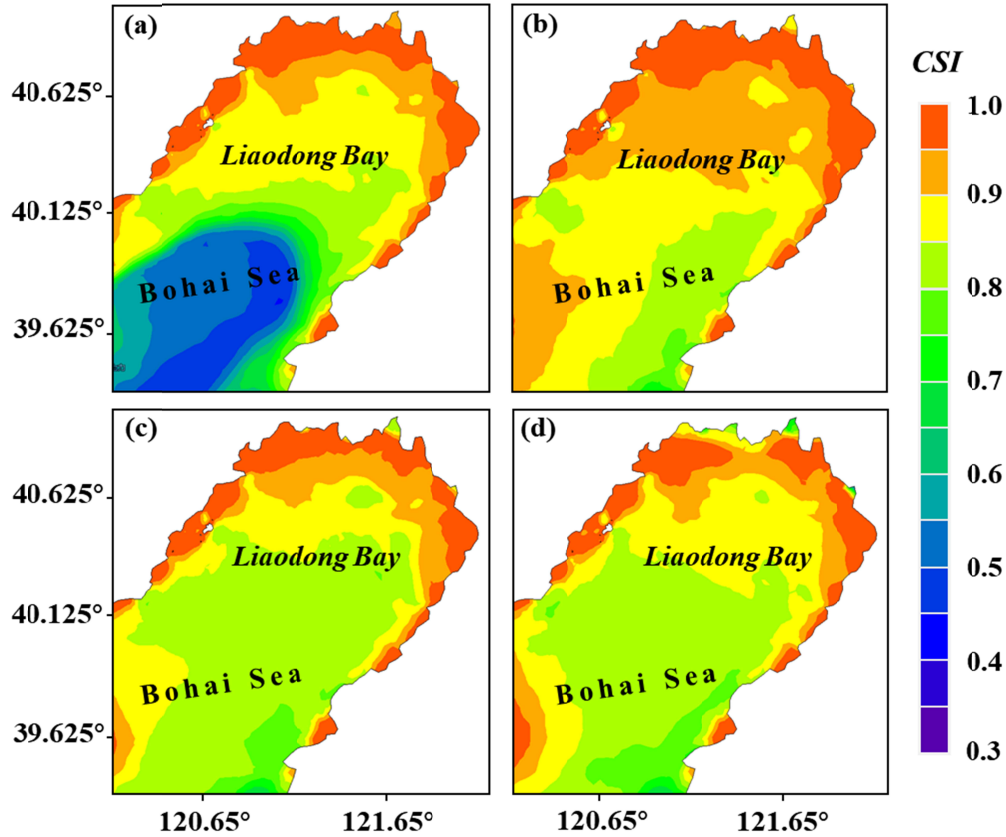


**Figure 7.** Distribution of the comprehensive suitability index ( *CSI* ) for stock enhancement of PTL during various periods in the Liaodong Bay. (a) Early June. (b) Late June. (c) Early July. (d) Late July.

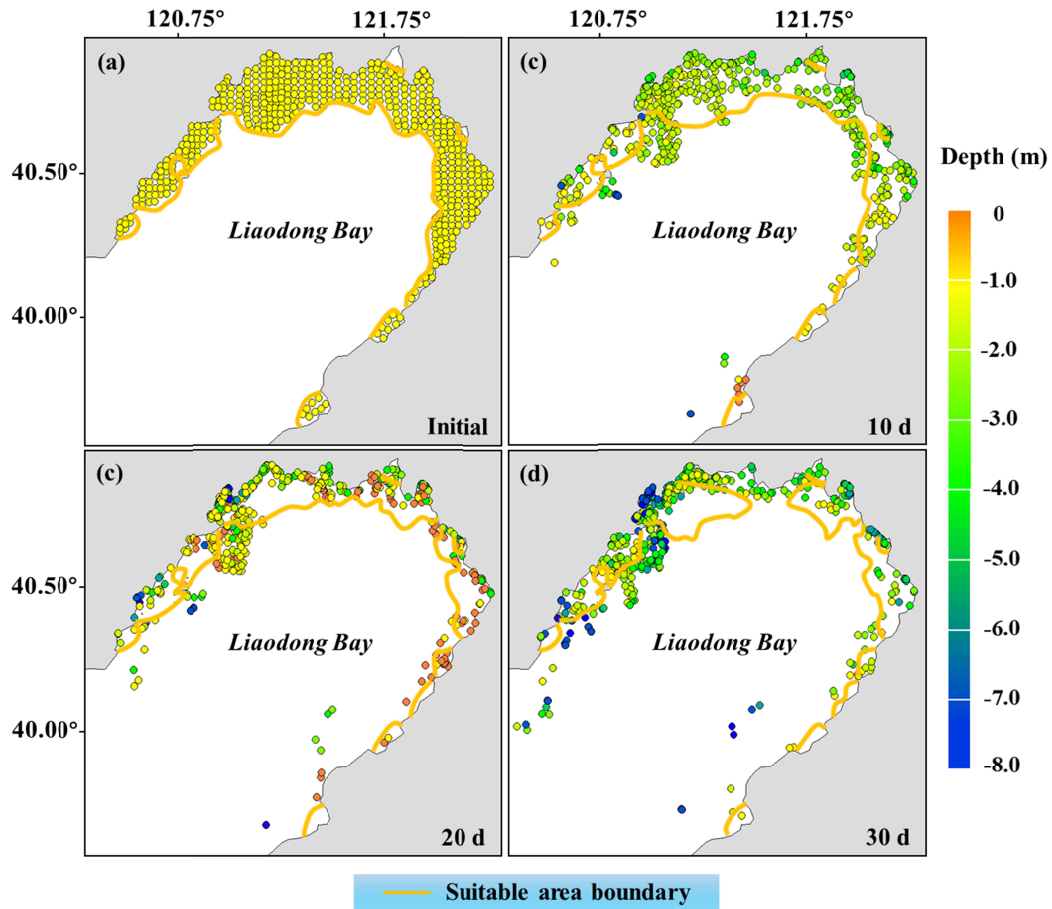
### 3.4 Migration characteristics of *Portunus trituberculatus* larvae (PTL)

After determining the initial suitable area, our interest lied in ascertaining the true survival rate of the larvae placed within it. This was because the distribution of the suitable area in real environments is subject to dynamic changes in environmental factors. Thus, it is crucial to determine whether the larvae will detach from the suitable area during the process of migration along with currents after being released.

Within the initial suitable area (Figure 7. (b) and Figure 8. (a)) identified by the habitat suitability model, larvae were released at even intervals of 2400 meters. The migration trajectory model subsequently predicted the migration positions of these

larvae on the 10th, 20th, and 30th days (Figure 8. (b), (c) and (d)). It should be noted that each larva represents the migratory characteristics within a range of 2400m x 2400m around its initial location. The results indicate that 10 days after release, the suitable area decreased, with 26.35% of PTL located outside the suitable area. The overall depth of larvae decreased compared to the initial time, with an average depth of about -2.12 m. After 20 days of release, PTL tended to aggregate in the nearshore area, with an average depth of about -0.89 m; approximately 32.67% of the larvae were located outside the suitable area at this time. When the larvae were released for 30 days, with the shrinking of the suitable area, more larvae were detached from it, accounting for approximately 46.81% of the total number of larvae.

The aforementioned observation implies that despite having selected regions with superior environmental suitability for stock enhancement and initial release, dynamic fluctuations in environmental conditions may cause the PTL to struggle to survive outside the favorable area. Therefore, our initial estimation of the suitable area may have been overestimated. In the light of this, we evaluated the actual available area for stock enhancement of PTL.



429

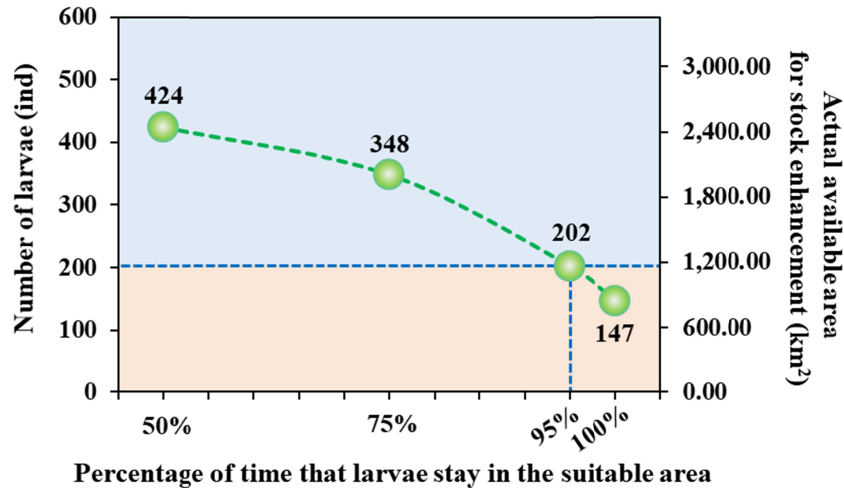
431 **Figure 8.** Migration location and distribution depth of PTL within 30 days after  
 432 release. (a) Early June. (b) Late June. (c) Early July. (d) Late July.

### 433 3.5 The actual available area for stock enhancement of *Portunus trituberculatus* 434 larvae (PTL)

440 In reality, the survival probability of the PTL is only greater when they stay  
 441 within the suitable habitat for a sufficiently long period of time. Here, we present a  
 442 joint water environment model and particle tracking model to evaluate the actual  
 443 suitable area for initial larvae release, by estimating the time that larvae stayed in the  
 444 suitable area within 30 days of release. Specifically, the probability of larvae escaping  
 445 from the suitable area after initial release indicates whether the surrounding area of  
 446 2400m×2400m around the initial location of the larvae is truly suitable for stock

enhancement. If the larvae stay in the suitable area for more than 95% of the time within 30 days after release, the area of 5.76 km<sup>2</sup> represented by the initial release location is considered as the true available area for natural proliferation of larvae and release of additionally reared ones.

For the purpose of quantification, we tabulated the total initial areas that can be utilized for larval stock enhancement when the proportion of time that larvae spend within the suitable area during a 30-day period reaches 50%, 75%, 95%, and 100%, respectively (Figure 9). The results indicate that a total of 424 larvae satisfied the condition of spending 50% of their time in the suitable area, corresponding to a viable area for growth and release of approximately 2442.24 km<sup>2</sup>, which represents 75.89% of the initial suitable area and 13.00% of the entire Liaodong Bay area. When the percentage of time spent in the suitable area was 75%, the available area for stock enhancement decreased to about 2004.48 km<sup>2</sup>, accounting for 62.29% of the initial suitable area and 10.67% of the entire Liaodong Bay. Nevertheless, when the percentage of time spent in the suitable area reached 95%, only 33.67% of larvae (202 individuals) met the conditions, and the actual available area for stock enhancement decreased to 1163.52 km<sup>2</sup>, which accounted for 36.16% of the initial suitable area and 6.19% of the entire Liaodong Bay. After being released at their initial area, 147 larvae remained within the suitable area throughout the entire observation period. The actual available area for stock enhancement was only 846.72 km<sup>2</sup>, accounting for 26.31% of the initial suitable area and 4.51% of the entire Liaodong Bay.



462

465 **Figure 9.** The relationship between the percentage of time that larvae stay in the  
 466 suitable area and the number of larvae as well as the actual available area for stock  
 467 enhancement.

#### 466 **4 Discussion**

479 In view of the importance of the marine environment for carrying out stock  
 480 enhancement, it was developed a comprehensive aquatic environmental model of the  
 481 Liaodong Bay. This model can simulate the bay temperature, salinity, tides, currents,  
 482 and wave characteristics. Based on a habitat suitability model, this study  
 483 comprehensively evaluated the environmental suitability of the Liaodong Bay during  
 484 the neap tide in June and July 2019, and identified suitable areas for the stock  
 485 enhancement of PTL. A combined analysis of habitat suitability and environmental  
 486 models demonstrates that flow velocity and water temperature in the Liaodong Bay  
 487 have significant effects on the growth of the PTL, while the effects of wave and  
 488 salinity are relatively minor. Previous studies have shown that there are significant  
 489 differences in water temperature among different seasons, which have also  
 490 constrained larvae distribution, and the implementation of stock enhancement and  
 491 release (Gilbert et al., 2010; Han et al., 2016; Lin and Nozawa, 2023; Nozawa, 2012;

479 Teodosio et al., 2016). Generally, water temperature in summer is significantly higher  
480 near the coast than in the open sea (Han and Wang, 2022; Yang et al., 2004). This  
481 study also confirms that suitability of water temperature in June and July exhibits  
482 different spatial distributions, with relatively higher temperature near the coast.  
483 Meanwhile, tidal and ocean currents are affected by the coastline and seafloor  
484 topography, showing considerable spatial variations.

485 Based on considerations of the success rate of the stock enhancement, this study  
486 employed a combination model to reveal the environmental suitability of PTL.  
487 Specifically, the study provides a reference for the suitable area and time for  
488 proliferation and release activities in the Liaodong Bay. In accordance with the results  
489 of this study, the optimal time for stock enhancement was found to be late June, when  
490 the largest area for implementation was available. The recommended stock  
491 enhancement sites were primarily concentrated in the northern waters of the Liaodong  
492 Bay and the coastal waters, with the areas near Jinzhou, Panjin, and Yingkou were  
493 identified as the best release locations within the study area (Ge, 2019; Wang et al.,  
494 2013). Additionally, it should be noted that different species have varying degrees of  
495 adaptability to environmental factors, thus suitable stock enhancement timing and  
496 locations should be selected based on the specific species in question.

497 Hydrodynamic models based on individual behavioral characteristics are widely  
498 used to predict larval transport (Christensen et al., 2008; Kim et al., 2010; Metaxas  
499 and Saunders, 2009; Zhong et al., 2023). The results of the migration model for PTL  
500 suggested that during their migration process, they move out of suitable areas and do  
501 not survive. This migration loss is inferred based on the assumption that the larvae  
502 lack autonomous swimming ability. As the larvae grow, they gradually acquire the  
503 ability to swim autonomously. Swimming behaviors could contribute significantly to



the overall larval transport potential since they are always responding to the stimuli provided by changes in depth (Baptista et al., 2019; Gallagher et al., 1996; Silva et al., 2016). Therefore, when considering the growth model of the larvae, it is necessary to take into account a certain period of time after they are released, which is one of the reasons why our migration trajectory model does not simulate a longer period of time. In addition, considering the characteristics of the larvae behaviour in pursuing food sources (Feehan et al., 2018; Fenaux et al., 1994), the abundance of food in the marine environment is a factor worth to be refined some time after the larvae were released. This study did not take into account the potential effects of food limitation on larvae, as food is generally abundant during the early stages of larval development.

Rational stock enhancement of aquatic organisms facilitate rebuilding conservation of fishery resources. The results of this study held significant implications for the management of offshore aquatic resources and ecological conservation. Furthermore, the proposed model and evaluation methods presented in this paper provided valuable references for the research of stock enhancement in other marine areas, and the selection of suitable habitats for marine organisms in general. These results contribute to the achievement of sustainable utilization of aquatic resources, and ecological conservation.

## **5 Conclusions**

The focus of this study identify the suitable environment stock enhancement of PTL in the Liaodong Bay. Firstly, the *HSI* of the basic environment factors (including tidal current, temperature, salinity and waves), was identified by combining the habitat environmental model and the habitat suitability model. The results indicated that the main limiting factors for the stock enhancement of PTL were flow velocity and water temperature, while waves were considered as a non-primary limiting factor

and were not considered in the calculation of the *CSI*. Secondly, the habitat suitability model showed that late June was the most suitable time to carry out the stock enhancement of PTL by considering multiple factors. The preliminary estimated suitable habitat area was 3,217.77 km<sup>2</sup>. Finally, based on the migration model of PTL, the deviation position of larvae leaving the suitable area and the actual available area for stock enhancement were further determined after releasing larvae within the initial suitable area. Only 33.67% of the larvae fulfilled the criteria of remaining within the suitable habitat for 95% of the time, resulting in an effective available area of 1,163.52 km<sup>2</sup> for stock enhancement purposes. This area accounts for 36.16% of the initial suitable habitat and 6.19% of the entire Liaodong Bay. This means that the actual area available for stock enhancement is likely to be a very small portion of the entire bay, and more precise release of larvae will be necessary to ensure survival rates after release. Based on these results, our study actually provides a methodological framework for the identification of suitable environment of stock enhancement as well. This methodology can provide technical guidance for the stock enhancement of marine larvae with same applicability for other bays, which in turn contributes to the sustainable use of marine ecosystem services and fisheries resources.

#### **Data Availability Statement**

The MIKE21-SW model is available due to the fact that Dalian Ocean University has purchased the rights to the software. Tide level data from two stations (S1, and S2) obtained from continuous 25-hour measurements on May 25, 2022, provided by the China National Marine Information Center; current data from three stations (C1, C2, and C3) measured using a current meter on September 18, 2021; water temperature and salinity from monthly average data from two stations (T1 and T2) for 2021, obtained from the Copernicus Marine Service website (<https://marine.copernicus.eu/>) product is: <https://doi.org/10.48670/moi-00021>; and wave data from one station

(W1), obtained from a fixed acoustic wave gauge over a 30-hour continuous observation period on May 14, 2016. Figures and analysis of the data were made with MATLAB version: 9.14.0 (R2023a). Water depth data can be download the International Bathymetric Chart of the Bohai sea Version 2 (IBCSO v2) ( Ma et al., 2021, <https://doi.org/10.1016/j.aquaculture.2021.736598>)

## Acknowledgements

The work was funded by the National Natural Science Foundation of China (Grant No. 31302232).

## References

- Baptista, V., Morais, P., Cruz, J., Castanho, S., Ribeiro, L., Pousao-Ferreira, P., Leitao, F., Wolanski, E., Teodosio, M.A. (2019). Swimming Abilities of Temperate Pelagic Fish Larvae Prove that they May Control their Dispersion in Coastal Areas. *Diversity-Basel*. 11(10). <https://doi.org/10.3390/d11100185>
- Blankenship, H.L., Leber, K.M. (1995). A Responsible Approach to Marine Stock Enhancement.
- Bolle, L.J., Dickey-Collas, M., van Beek, J.K.L., Erftemeijer, P.L.A., Witte, J.I.J., van der Veer, H.W., Rijnsdorp, A.D. (2009). Variability in Transport of Fish Eggs and Larvae. Iii. Effects of Hydrodynamics and Larval Behaviour On Recruitment in Plaice. *Marine Ecology Progress Series*. 390, 195-211. <https://doi.org/10.3354/meps08177>
- China, M.O.A.O., 2014. Technical Specifications for the Stock Enhancement of Hydrobios—*Portunus Trituberculatus*.
- Christensen, A., Jensen, H., Mosegaard, H., John, M.S., Schrum, C. (2008). Sandeel (Ammodytes Marinus) Larval Transport Patterns in the North Sea From an Individual-Based Hydrodynamic Egg and Larval Model. *Canadian Journal of Fisheries and Aquatic Sciences*. 65(7), 1498-1511. <https://doi.org/10.1139/F08-073>
- Christou, P., Savin, R., Costa-Pierce, B.A., Misztal, I., Whitelaw, C.B.A., 2013. Marine Fisheries Enhancement: Coming of Age in the New Millennium, in: Christou, P., Savin, R., Costa-Pierce, B.A., Misztal, I., Whitelaw, C.B.A. (Eds.), Sustainable Food Production, Christou, P., Savin, R., Costa-Pierce, B.A., Misztal, I., Whitelaw, C.B.A. ed. Springer Science+Business Media.
- Colloca, F., Cardinale, M., Maynou, F., Giannoulaki, M., Scarcella, G., Jenko, K., Maria Bellido, J., Fiorentino, F. (2013). Rebuilding Mediterranean Fisheries: A New Paradigm for Ecological Sustainability. *Fish and Fisheries*. 14(1), 89-109. <https://doi.org/10.1111/j.1467-2979.2011.00453.x>
- Dai, C., Wang, F., Fang, Z., Dong, S. (2014). Effects of Temperature On the Respiratory Metabolism and Activities of Related Enzymes of Swimming Crab Portunus Trituberculatus. *PROGRESS FISHERY SCIENCES*. 35(2), 90-96. <https://doi.org/10.3969/j.issn.1000-7075.2014.02.013>
- Dong, J., Jiang, L.X., Tan, K.F., Liu, H.Y., Purcell, J.E., Ye, L. (2009). Stock Enhancement of the

593 Edible Jellyfish ( *Rhopilema Esculentum* Kishinouye) in Liaodong Bay, China: A Review.  
594 *Hydrobiologia*. 1(616), 113-118.

595 Etiegni, C.A., Ostrovskaya, E., Leentvaar, J., Eizinga, F. (2011). Mitigation of Illegal Fishing Activities:  
596 Enhancing Compliance with Fisheries Regulation in Lake Victoria (Kenya). *Regional*  
597 *Environmental Change*. 11(2), 323-334. <https://doi.org/10.1007/s10113-010-0134-4>

598 Feehan, C.J., Grauman-Boss, B.C., Strathmann, R.R., Dethier, M.N., Duggins, D.O. (2018). Kelp  
599 Detritus Provides High-Quality Food for Sea Urchin Larvae. *Limnology and Oceanography*. 63,  
600 S299-S306. <https://doi.org/10.1002/lno.10740>

601 Fenaux, L., Strathmann, M.F., Strathmann, R.R. (1994). 5 Tests of Food-Limited Growth of Larvae in  
602 Coastal Waters by Comparisons of Rates of Development and Form of Echinoplutei. *Limnology*  
603 *and Oceanography*. 39(1), 84-98. <https://doi.org/10.4319/lo.1994.39.1.0084>

604 Gallagher, S.M., Manuel, J.L., Manning, D.A., ODor, R. (1996). Ontogenetic Changes in the Vertical  
605 Distribution of Giant Scallop Larvae, *Placopecten Magellanicus*, in 9-M Deep Mesocosms as a  
606 Function of Light, Food, and Temperature Stratification. *Marine Biology*. 124(4), 679-692.  
607 <https://doi.org/10.1007/BF00351049>

608 Gao, L., Bai, X., Wang, Y. (2022). Dynamic Prediction of the Ricker-Type Model of *Portunus*  
609 *Trituberculatus* On the Basis of Marine Environmental Factors. *Frontiers in Marine Science*. 9.  
610 <https://doi.org/10.3389/fmars.2022.850317>

611 Ge, Y., 2019. Study On the Stocking and Release of *Portunus Trituberculatus* in Panjin Area of  
612 Northern Liaodong Bay. Dalian Ocean University.  
613 <https://doi.org/10.27821/d.cnki.gdlhy.2019.000049>

614 Gilbert, C.S., Gentleman, W.C., Johnson, C.L., DiBacco, C., Pringle, J.M., Chen, C. (2010). Modelling  
615 Dispersal of Sea Scallop (*Placopecten Magellanicus*) Larvae On Georges Bank: The Influence of  
616 Depth-Distribution, Planktonic Duration and Spawning Seasonality. *Progress in Oceanography*.  
617 57(1-4), 37-48. <https://doi.org/10.1016/j.pocean.2010.09.021>

618 Green, A.L., Fernandes, L., Almany, G., Abesamis, R., McLeod, E., Alino, P.M., White, A.T., Salm, R.,  
619 Tanzer, J., Pressey, R.L. (2014). Designing Marine Reserves for Fisheries Management,  
620 Biodiversity Conservation, and Climate Change Adaptation. *Coastal Management*. 42(2), 143-159.  
621 <https://doi.org/10.1080/08920753.2014.877763>

622 Han, Q.X., Keesing, J.K., Liu, D.Y. (2016). A Review of Sea Cucumber Aquaculture, Ranching, and  
623 Stock Enhancement in China. *Reviews in Fisheries Science & Aquaculture*. 24(4), 326-341.  
624 <https://doi.org/10.1080/23308249.2016.1193472>

625 Han, S., Wang, Z., (2022). Simulation of Seasonal Variation Characteristics of Offshore Water  
626 Temperature Based On Roms Model, 2022 Global Reliability and Prognostics and Health  
627 Management (PHM-Yantai).

628 Hilborn, R., Amoroso, R.O., Anderson, C.M., Baum, J.K., Branch, T.A., Costello, C., de Moor, C.L.,  
629 Faraj, A., Hively, D., Jensen, O.P., Kurota, H., Little, L.R., Mace, P., McClanahan, T., Melnychuk,  
630 M.C., Minto, C., Osio, G.C., Parma, A.M., Pons, M., Segurado, S., Szuwalski, C.S., Wilson, J.R.,  
631 Ye, Y. (2020). Effective Fisheries Management Instrumental in Improving Fish Stock Status.  
632 *Proceedings of the National Academy of Sciences of the United States of America*. 117(4),

2218-2224. <https://doi.org/10.1073/pnas.1909726116>

Hong, W., Zhang, Q. (2002). Artificial Propagation and Breeding of Marine Fish in China. *Chinese Journal of Oceanology and Limnology*. 20(1), 41-51.

Horodysky, A.Z., Cooke, S.J., Graves, J.E., Brill, R.W. (2016). Themed Issue Article: Conservation Physiology of Marine Fishes Fisheries Conservation On the High Seas: Linking Conservation Physiology and Fisheries Ecology for the Management of Large Pelagic Fishes. *Conservation Physiology*. 4. <https://doi.org/10.1093/conphys/cov059>

Hou, W., Liang, S., Hu, X., Li, C., Sun, Z., Ma, Q. (2022). Ecological Characteristics of a Typical Coastal Artificial Shoreline Considering the Key Drivers Involved. *Estuarine Coastal and Shelf Science*. 277. <https://doi.org/10.1016/j.ecss.2022.108069>

Hou, W., Zhang, R., Xi, Y., Liang, S., Sun, Z. (2020). The Role of Waterlogging Stress On the Distribution of Salt Marsh Plants in the Liao River Estuary Wetland. *Global Ecology and Conservation*. 23. <https://doi.org/10.1016/j.gecco.2020.e01100>

Hou, W., Zhang, R., Zhang, P., Xi, Y., Ma, Q. (2021). Wave Characteristics and Berthing Capacity Evaluation of the Offshore Fishing Port Under the Influence of Typhoons. *Applied Ocean Research*. 106. <https://doi.org/10.1016/j.apor.2020.102447>

Karydis, M., Kitsiou, D. (2013). Marine Water Quality Monitoring: A Review. *Marine Pollution Bulletin*. 77(1-2), 23-36. <https://doi.org/10.1016/j.marpolbul.2013.09.012>

Kim, C., Park, K., Powers, S.P., Graham, W.M., Bayha, K.M. (2010). Oyster Larval Transport in Coastal Alabama: Dominance of Physical Transport Over Biological Behavior in a Shallow Estuary. *Journal of Geophysical Research-Oceans*. 115. <https://doi.org/10.1029/2010JC006115>

Kitada, S. (2014). Japanese Chum Salmon Stock Enhancement: Current Perspective and Future Challenges. (Special Features: Social-Ecological Systems On Walleye Pollock Under Changing Environment: Inter-Disciplinary Approach.). *Fisheries Science*. 80(2), 237-249.

Laroche, J., Boudry, P., Charrier, G., Morvezen, R. (2016). Stock Enhancement Or Sea Ranching? Insights From Monitoring the Genetic Diversity, Relatedness and Effective Population Size in a Seeded Great Scallop Population (*Pecten Maximus*). *Heredity: An International Journal of Genetics*.

Lee, H., Chang, Y., Liao, C., Hsu, T. (2022). Development of Integrated Multitrophic Aquaculture-Based Cage Rearing System in an Underutilized Fishing Port and its Application in Marine Stock Enhancement. *Frontiers in Marine Science*. 9. <https://doi.org/10.3389/fmars.2022.998198>

Lin, C., Nozawa, Y. (2023). The Influence of Seawater Temperature On the Timing of Coral Spawning. *Coral Reefs*. <https://doi.org/10.1007/s00338-023-02349-9>

Lorenzen, K., Leber, K.M., Blankenship, H.L. (2010). Responsible Approach to Marine Stock Enhancement: An Update. *Reviews In Fisheries Science*. 18(2), 189-210. <https://doi.org/10.1080/10641262.2010.491564>

Ma, Q., Han, Y., Xi, Y., Huang, J., Sheng, Z., Zhang, R. (2021). Prediction Study On the Spatiotemporal Distribution of Yesso Scallop Larvae Based On a Coupled Biophysical Model. *Aquaculture*. 539, 736598. <https://doi.org/https://doi.org/10.1016/j.aquaculture.2021.736598>

673 Ma, Q., Liang, S., Sun, Z., Zhang, R., Wang, P. (2023). Development and Evaluation of a Gpu-Based  
674 Coupled Three-Dimensional Hydrodynamic and Water Quality Model. *Marine Pollution Bulletin*.  
675 187. <https://doi.org/10.1016/j.marpolbul.2022.114494>

676 McGeady, R., Lordan, C., Power, A.M. (2021). Shift in the Larval Phenology of a Marine Ectotherm  
677 Due to Ocean Warming with Consequences for Larval Transport. *Limnology and Oceanography*.  
678 66(2), 543-557. <https://doi.org/10.1002/lno.11622>

679 Metaxas, A., Saunders, M. (2009). Quantifying the "Bio-" Components in Biophysical Models of  
680 Larval Transport in Marine Benthic Invertebrates: Advances and Pitfalls. *Biological Bulletin*.  
681 216(3), 257-272. <https://doi.org/10.1086/BBLv216n3p257>

682 Nielsen, K.N., Holm, P. (2007). A Brief Catalogue of Failures: Framing Evaluation and Learning in  
683 Fisheries Resource Management. *Marine Policy*. 31(6), 669-680.  
684 <https://doi.org/10.1016/j.marpol.2007.03.014>

685 Nozawa, Y. (2012). Annual Variation in the Timing of Coral Spawning in a High-Latitude  
686 Environment: Influence of Temperature. *Biological Bulletin*. 222(3), 192-202.  
687 <https://doi.org/10.1086/BBLv222n3p192>

688 Nurdiani, R., Zeng, C. (2007). Effects of Temperature and Salinity On the Survival and Development  
689 of Mud Crab, *Scylla Serrata* (Forsskal), Larvae. *Aquaculture Research*. 38(14), 1529-1538.  
690 <https://doi.org/10.1111/j.1365-2109.2007.01810.x>

691 Pilnick, A.R., O'Neil, K.L., Moe, M., Patterson, J.T. (2021). A Novel System for Intensive Diadema  
692 Antillarum Propagation as a Step Towards Population Enhancement. *Scientific Reports*. 11(1).  
693 <https://doi.org/10.1038/s41598-021-90564-1>

694 Purcell, S.W., Hair, C.A., Mills, D.J. (2012). Sea Cucumber Culture, Farming and Sea Ranching in the  
695 Tropics: Progress, Problems and Opportunities. *Aquaculture*. 368-369(Complete), 68-81.

696 Reidenbach, M.A., Koseff, J.R., Koehl, M.A.R. (2009). Hydrodynamic Forces On Larvae Affect their  
697 Settlement On Coral Reefs in Turbulent, Wave-Driven Flow. *Limnology and Oceanography*. 54(1),  
698 318-330. <https://doi.org/10.4319/lo.2009.54.1.0318>

699 Roberts, C.M., Hawkins, J.P., Gell, F.R. (2005). The Role of Marine Reserves in Achieving  
700 Sustainable Fisheries. *Philosophical Transactions of the Royal Society B-Biological Sciences*.  
701 360(1453), 123-132. <https://doi.org/10.1098/rstb.2004.1578>

702 Shanks, A.L., Largier, J., Brubaker, J. (2003). Observations On the Distribution of Meroplankton  
703 During an Upwelling Event. *Journal of Plankton Research*. 25(6), 645-667.  
704 <https://doi.org/10.1093/plankt/25.6.645>

705 Shelbourne, J.E. (1964). The Artificial Propagation of Marine Fish. *Advances in Marine Biology*. 2,  
706 1-83.

707 Silva, C.S.E., Novais, S.C., Lemos, M.F.L., Mendes, S., Oliveira, A.P., Goncalves, E.J., Faria, A.M.  
708 (2016). Effects of Ocean Acidification On the Swimming Ability, Development and Biochemical  
709 Responses of Sand Smelt Larvae. *Science of the Total Environment*. 563, 89-98.  
710 <https://doi.org/10.1016/j.scitotenv.2016.04.091>

711 Skålvik, A.M., Sætre, C., Frøysa, K., Bjørk, R., Tengberg, A. (2023). Challenges, Limitations, and  
712 Measurement Strategies to Ensure Data Quality in Deep-Sea Sensors. *Frontiers in Marine Science*.

10. <https://doi.org/10.3389/fmars.2023.1152236>

Taylor, M.D., Palmer, P.J., Fielder, D.S., Suthers, I.M. (2005). Responsible Estuarine Finfish Stock Enhancement: An Australian Perspective. *Journal of Fish Biology*. 67(2), 299-331. <https://doi.org/10.1111/j.0022-1112.2005.00809.x>

Teodosio, M.A., Paris, C.B., Wolanski, E., Morais, P. (2016). Biophysical Processes Leading to the Ingress of Temperate Fish Larvae Into Estuarine Nursery Areas: A Review. *Estuarine Coastal and Shelf Science*. 183, 187-202. <https://doi.org/10.1016/j.ecss.2016.10.022>

Utomo, A.D., Wibowo, A., Suhaimi, R.A., Atminarso, D., Baumgartner, L.J. (2019). Challenges Balancing Fisheries Resource Management and River Development in Indonesia. *Marine and Freshwater Research*. 70(9), 1265-1273. <https://doi.org/10.1071/MF19160>

Uzun, P., Farazande, S., Guven, B. (2022). Mathematical Modeling of Microplastic Abundance, Distribution, and Transport in Water Environments: A Review. *Chemosphere*. 288. <https://doi.org/10.1016/j.chemosphere.2021.132517>

Wang, B., Liu, X., Li, Y., Dong, J., Wang, A., Yu, X., Wang, X., Li, C., Luan, C., Wang, Y. (2020). Stocking Effectiveness of Hatchery-Raised Swimming Crabs (*Portunus Trituberculatus*) Released Into Liaodong Bay. *Journal of Fisheries of China*. 44(8), 11. <https://doi.org/10.11964/jfc.20190811903>

Wang, B., Qin, Y., Dong, J., Li, Y., Wang, W., Li, Y., Sun, M., Liu, C. (2013). Dynamic Distribution of *Nemopilema Nomurai* in Inshore Waters of the Northern Liaodong Bay, Bohai Sea. *Acta Ecologica Sinica*. 33(6), 1701-1712.

Wang, J., Liu, Q., Zhang, X., Gao, G., Niu, M., Wang, H., Chen, L., Wang, C., Mu, C., Wang, F. (2022). Metabolic Response in the Gill of *Portunus Trituberculatus* Under Short-Term Low Salinity Stress Based On Gc-Ms Technique. *Frontiers in Marine Science*. 9. <https://doi.org/10.3389/fmars.2022.881016>

Wang, Y., Gao, L., Chen, Y. (2018). Assessment of *Portunus (Portunus) Trituberculatus* (Miers, 1876) Stock in the Northern East China Sea. *Indian Journal of Fisheries*(65-4).

Wang, Y., Wang, X., Ye, T., Chen, L., Zhou, C. (2017). Spawner-Recruit Analysis of *Portunus (Portunus) Trituberculatus* (Miers, 1876) in the Case of Stock Enhancement Implementation: A Case Study in Zhejiang Sea Area, China. *Turkish Journal of Fisheries and Aquatic Sciences*. 17(2), 293-299.

Wang, Z., Feng, J., Lozano-Montes, H.M., Loneragan, N.R., Zhang, X., Tian, T., Wu, Z. (2022). Estimating Ecological Carrying Capacity for Stock Enhancement in Marine Ranching Ecosystems of Northern China. *Frontiers in Marine Science*. 9. <https://doi.org/10.3389/fmars.2022.936028>

Wang, Z., Sun, P., Wang, L., Zhang, M., Wang, Z. (2021). Monitoring Sea Ice in Liaodong Bay of Bohai Sea During the Freezing Period of 2017/2018 Using Sentinel-2 Remote Sensing Data. *Journal of Spectroscopy*. 2021. <https://doi.org/10.1155/2021/9974845>

Whitman, E.R., Reidenbach, M.A. (2012). Benthic Flow Environments Affect Recruitment of *Crassostrea Virginica* Larvae to an Intertidal Oyster Reef. *Marine Ecology Progress Series*. 463, 177-191. <https://doi.org/10.3354/meps09882>

Xie, Z., Qiu, S., Hou, C., Jin, X. (2014). Recapture Rates of Swimming Crabs(*Portunus Trituberculatus*)

Released in the Waters Off Southern Shandong Peninsula. *Journal of Fishery Sciences of China*.  
 21(5), 10.

Xu, Q., Liu, Y. (2011). Gene Expression Profiles of the Swimming Crab *Portunus Trituberculatus*  
 Exposed to Salinity Stress. *Marine Biology*. 158(10), 2161-2172.  
<https://doi.org/10.1007/s00227-011-1721-8>

Xu, S., Song, J., Duan, L., Wu, X., Xu, Y. (2010). Structural Changes of Major Fishery Resources in  
 the Bohai Sea. *Marine Sciences*. 34(6), 59-65.

Yang, D., Gao, Z., Chen, Y., Wang, P., Sun, P. (2004). Influence of Seawater Temperature On  
 Phytoplankton Growth in Jiaozhou Bay, China. *Chinese Journal of Oceanology and Limnology*.  
 22(2), 166-175.

Yoshimura, K., Hagiwara, A., Yoshimatsu, T., Kitajima, C. (1996). Culture Technology of Marine  
 Rotifers and the Implications for Intensive Culture of Marine Fish in Japan. *Mar.Freshwater Res.*  
 47(2), 217-222.

Zhong, Y., Zhang, J., Song, D., Zhao, Y., Liu, Y., Wu, W., Qiao, L. (2023). Numerical Study of  
 Hydrodynamic Effects On Manila Clam Population Distribution and Transport in the Southwest  
 Laizhou Bay, China. *Science of the Total Environment*. 865.  
<https://doi.org/10.1016/j.scitotenv.2022.161214>

Zimmerman, K.M., Pechenik, J.A. (1991). How Do Temperature and Salinity Affect Relative Rates of  
 Growth, Morphological-Differentiation, and Time to Metamorphic Competence in Larvae of the  
 Marine Gastropod *Crepidula-Plana*. *Biological Bulletin*. 180(3), 372-386.  
<https://doi.org/10.2307/1542338>